Mice lacking angiotensin type 2 receptor exhibit a sex-specific attenuation of insulin sensitivity

Diego T. Quiroga[1], **Johanna G. Miquet**[1], **Lorena Gonzalez**[1], **Ana I. Sotelo**[1], **Marina C. Muñoz**[1], **Pedro M. Geraldes**[2,3], **Jorge F. Giani**[4], **Fernando P. Dominici**[1]

[1]Universidad de Buenos Aires, Facultad de Farmacia y Bioquímica, Departamento de Química Biológica, IQUIFIB (UBA-CONICET), Buenos Aires, Argentina.

[2]Research Center of the CHU de Sherbrooke, Université de Sherbrooke, Sherbrooke, Québec, Canada.

[3]Division of Endocrinology, Department of Medicine, Université de Sherbrooke, Sherbrooke, Québec, Canada.

[4]Department of Biomedical Sciences, Cedars-Sinai Medical Center, Los Angeles, California, USA.

Abstract

The renin-angiotensin system modulates insulin action. Pharmacological stimulation of angiotensin type 2 receptor (AT2R) was shown to have beneficial metabolic effects in various animal models of insulin resistance and type 2 diabetes and also to increase insulin sensitivity in wild type mice. In this study we further explored the role of the AT2R on insulin action and glucose homeostasis by investigating the glycemic profile and in vivo insulin signaling status in insulin-target tissues from both male and female AT2R knockout (KO) mice. When compared to the respective wild-type (WT) group, glycemia and insulinemia was unaltered in AT2RKO mice regardless of sex. However, female AT2RKO mice displayed decreased insulin sensitivity compared to their WT littermates. This was accompanied by a compensatory increase in adiponectinemia and with a specific attenuation of the activity of main insulin signaling components (insulin receptor, Akt and ERK1/2) in adipose tissue with no apparent alterations in insulin signaling in either liver or skeletal muscle. These parameters remained unaltered in male AT2RKO mice as compared to male WT mice. Present data show that the AT2R has a physiological role in the conservation of insulin action in female but not in male mice. Our results suggest a sexual dimorphism in the control of insulin action and glucose homeostasis by the AT2R

and reinforce the notion that pharmacological modulation of the balance between the AT1R and AT2R receptor could be important for treatment of metabolic syndrome and type 2 diabetes.

Keywords

Angiotensin type 2 receptor; Adiponectin; Insulin signaling; Insulin sensitivity; Knockout mice; Renin-angiotensin system

Introduction

The renin-angiotensin system (RAS) is a complex hormonal cascade of major importance in the pathophysiology of hypertension. Angiotensin (Ang) II is a key hormone in the RAS, with pleiotropic actions (Forrester et al., 2018). This octapeptide binds with high affinity to two G protein-coupled receptors, the angiotensin type-1 receptor (AT1R) and the angiotensin type-2 receptor (AT2R) (Karnik et al., 2015). Most of the actions of Ang II, including vasoconstriction, antinatriuresis, aldosterone secretion and sympathetic nervous system activation, cellular dedifferentiation and growth, inflammation, and target organ damage among other detrimental actions are mediated by the AT1R (Forrester et al., 2018; Karnik et al., 2015). Although the physiological functions of the AT2R are less known, in general, interaction of the AT2R with Ang II or more recently characterized peptides of the RAS such as angiotensin-(1–7), generates actions that oppose those generated through AT1R activation (Carey, 2017; Matavelli and Siragy, 2015; Santos et al., 2019). The AT2R, while being only sparsely expressed in most healthy tissues (Forrester et al., 2018; Karnik et al., 2015; Shao et al., 2013), is strongly upregulated following tissue damage (Steckelings et al., 2010) such as vascular (Nakajima et al., 1995), and neuronal injury (Gallinat et al., 1998), myocardial infarction (Altarche-Xifró et al., 2009; Busche et al., 2000; Nio et al., 1995) and brain ischemia (Li et al., 2005). The selective stimulation of the AT2R with a recently available small-molecule ligand, compound 21 (C21), has not only greatly helped to elucidate the major molecular pathways involved in AT2R-mediated tissue protection, such as anti-inflammation, anti-fibrosis and anti-apoptosis, but has also revealed a great potential for pharmacological intervention in the above-mentioned diseases (Santos et al., 2019).

Angiotensin II is involved in the development of insulin resistance (Saiki et al., 2009). Chronic elevation of Ang II impairs insulin sensitivity and leads to development of insulin resistance. In various animal models of insulin resistance and/or type 2-diabetes, blockade of the AT1R consistently improves insulin sensitivity and glucose homeostasis (Henriksen et al., 2001; Muñoz et al., 2009; Rodriguez et al., 2018; Shiuchi et al., 2004).

Unlike the AT1R, the role of the AT2R in metabolism is not yet defined, but accumulated data indicates that it could have a positive role on insulin action. Acute systemic blockade of AT2R with PD123319, has been shown to decrease skeletal muscle glucose uptake in rats (Chai et al., 2010; 2011) and to impair insulin secretion in mice (Leung et al., 2014). In line with these results, we have demonstrated that chronic treatment with PD123319 exerts a negative modulation on insulin signaling (Muñoz et al., 2017). Importantly, administration of C21 exerts a beneficial effect on insulin sensitivity in both diabetic and insulin resistant animal models (Ohshima et al., 2012; Shao et al., 2013; Shao et al., 2014; Than et al., 2017;

Wang et al., 2017). In addition, administration of C21 has recently been shown to enhance insulin delivery and metabolic action in rat skeletal muscle (Yan et al., 2018) and we have recently shown that prolonged treatment with C21 enhances insulin sensitivity mice (Quiroga et al., 2018). These observations support the potential role of AT2R as a modulator of insulin action and glucose homeostasis.

Remarkably, unlike results obtained from AT2R stimulation or antagonism, information obtained from AT2R knockout (KO) mice has not been consistent so far (Noll et al., 2015; Samuel et al., 2013; Shiuchi et al., 2004; Yvan-Charvet et al., 2005). In brief, AT2RKO mice have reported to show decreased glucose transport in adipose tissue (Shiuchi et al., 2004), increased insulin sensitivity (Yvan-Charvet et al., 2005), and more recently insulin resistance in female mice without changes in male mice (Samuel et al., 2013), as compared to hyperglycemia and reduced insulin levels in male AT2RKO mice (Noll et al., 2015).

With the objective of further characterizing the role of AT2R in glucose homeostasis, our current work analyzed the phenotype of both male and female AT2R knockout mice in terms of metabolic parameters, insulin and glucose tolerance tests, as well as the status of insulin signaling in the main insulin target tissues. We found that female AT2RKO displayed decreased insulin sensitivity as compared to wild-type (WT) controls. This was accompanied by decreased insulin-mediated IR and Akt activation in liver and adipose tissue. In contrast, the phenotype of male AT2RKO mice regarding these parameters was unaltered when compared to WT control animals. Collectively, we provide evidence for a decline of insulin action in AT2RKO mice that seems to be both sex- and tissue-specific.

2. Materials and Methods

2.1. Materials

The rabbit polyclonal anti-insulin receptor (IR) β-subunit (C19; sc-711), the mouse monoclonal anti-phosphotyrosine (PY99; sc-7020), the goat polyclonal anti-rabbit IgG conjugated with HRP (sc-2004), the goat anti-mouse IgG-HRP (sc-2005) and rabbit anti-goat IgG-HRP (sc-2768) antibodies were purchased from Santa Cruz Biotechnology, Inc. (Santa Cruz, CA, USA). The rabbit polyclonal antibody anti-phospho-Akt-S473 (4060), the rabbit polyclonal antibody anti-phospho-Akt-T308 (9275), the anti-Akt (pan) rabbit monoclonal antibody (C67E7) that detects endogenous levels of total AKT1, AKT2, and AKT3 protein, the rabbit monoclonal, the rabbit monoclonal antibody anti-phospho-ERK1/2, that detects ERK-1 and −2 (p44 and p42 MAPK respectively) when phosphorylated at T202 and Y204 (4370) and the rabbit polyclonal antibody anti-ERK1/2 (9102) were from Cell Signalling (Danvers, MA, USA). The goat polyclonal anti-adiponectin (AF1119) antibody was from R&D systems (Minneapolis, MN, USA). The rabbit polyclonal antibody anti-UCP-1 (PA1–24894 was from Thermo Fisher (Rockford, IL, USA). Protein loading in the gels was evaluated with a polyclonal anti-actin antibody produced in rabbit (Sigma-Aldrich, USA, Catalog Number A2066).

2.2 Experimental animals

Mice hemizygous for targeted disruption of the Agtr2 gene (AT2RKO) were generated by Prof. Tadashi Inagami (Department of Biochemistry, Nashville University, Nashville, TN, USA; Ichiki et al., 1995). AT2RKO mice on a C57BL/6 genetic background, were generated by mating male AT2RKO mice with female wild-type C57BL/6 mice (Charles River, Montreal, QC, Canada). Because the Agtr2 gene is on the X chromosome and embryonic stem cells are XY, all F1 male mice were wild type (WT) and all F1 females were heterozygous for the mutation. These heterozygous females were mated with F1 males, giving rise to an F2 generation that included homozygous male and littermate controls. The homozygous males were healthy and fertile. As for female, homozygous was created by mating F2 male AT2R-KO with F1 female heterozygous. Age-matched control female mice were obtained during the F1 female heterozygous and the F1 male breeding strategy. RNA from homozygous males was analyzed by northern blotting to confirm the absence of AT2R transcripts that are normally expressed at high levels in fetuses and in adult brains (Ichiki et al., 1995). Male and female AT2RKO mice from our colony and the respective WT mice (Charles River, Montreal, QC, Canada) were housed in a specific pathogen-free facility with a temperature-controlled room and regulated with a 12:12-h light-dark cycle with free access to water and food containing 6% fiber, 23% protein and 4.5% fat. (Rodent laboratory chow 5001, Purina, St-Louis, MO, USA). Animal experiments comply with the ARRIVE guidelines and were performed in accordance with the guidelines of the Canadian Council on Animal Care and the National Institutes of Health guide for the care and use of Laboratory animals (NIH Publications No. 8023, revised 1978). In addition, all the procedures were approved by the Animal Care and Ethics Committee of the Faculty of Medicine and Health Sciences of the Universite de Sherbrooke.

2.3 Glucose and Insulin Tolerance Tests

At 10 weeks of age, 6 mice from each group were assessed for glucose tolerance and insulin tolerance. Animals were fasted for 6 h (8:00 AM-14:00 PM) prior to beginning of the GTT. Baseline glucose levels were sampled from tail blood using a commercial glucometer (Accu-Check,Roche Diagnostics Corp., Indianapolis, IN). Then, mice were injected I.P with 2 g of glucose per kilogram of body weight (BW) using a 20% glucose solution (w/v). and blood glucose was measured at 15, 30, 60, and 120 min post-injection. After a 2-day interval, mice were subjected to an insulin tolerance test (ITT). After a 6 h fast, mice were injected I.P. with 1 IU porcine insulin (Sigma-Aldrich) per kilogram of body weight. Blood glucose was measured at 0, 15, 30, 45, 60, and 120 min. Data for GTT is presented as absolute values, while that for ITT is presented as % of initial blood glucose levels.

2.4 Acute Insulin Stimulation and Tissue Collection

At 11 weeks of age, mice were fasted for 6 h (8:00 AM-14:00 PM) and anesthetized by the i.p. administration of a mixture of ketamine and xylazine (50 and 1 mg/kg, respectively). After anesthesia was guaranteed by the loss of pedal and corneal reflexes, the abdominal cavity was opened, and a dose of insulin previously demonstrated to attain maximal stimulation of the insulin receptor (10 IU porcine insulin/kg BW) dissolved in 0.2 ml of normal saline (0.9% NaCl) was injected via the vena cava. Baseline values were obtained by

studying another group of mice that injected with vehicle only. The liver, adipose tissue (perigonadal), and skeletal muscle (hindlimb), were removed after 1, 3, and 6 min, respectively. Serum was obtained from blood of saline-injected animals by centrifugation (3200 g for 10 min at 4 °C). Tissues and an aliquot of serum (for insulin and adiponectin determination) were kept at −80°C until analysis. Another aliquot of serum was used for determination of circulating triglyceride and cholesterol concentrations.

2.5. Tissue protein solubilization and immunoprecipitation

Tissue samples were homogenized in ice-cold homogenization buffer containing 1% Triton together with phosphatase and protease inhibitors, (1g of tissue/ml) as described previously (Muñoz et al., 2009; 2017; Quiroga et al., 2018). Tissue extracts were centrifuged at 100,000 g for 1 h at 4°C to eliminate insoluble material, and protein concentration in the supernatants was measured using the bicinchoninic acid assay (Pierce BCA Protein Assay Reagent; Thermo Scientific, Waltham, MA, USA). Samples were normalized for protein content, mixed with 2X Laemli buffer and kept at −20° C until electrophoresis was performed. For immunoprecipitation, equal amounts of tissue extracts (2 mg total protein in a final volume of 0.2 ml) were incubated overnight at 4° C with an anti-IR antibody directed against the IR β-subunit at a final concentration of 4 mg/ml. After incubation, 20 μl protein A-Sepharose 50% v/v in homogenization buffer were added to the mixture. Additional samples were incubated in the absence of immunoprecipitating antibody to corroborate that the precipitated proteins were specifically recognized by the immunoprecipitating antibody and not by protein A-Sepharose. The preparation was further incubated for 2 h at 4°C. After spin centrifugation, the supernatant was eliminated and the precipitate was washed three times with buffer containing 50 mM Tris, 10 mM sodium vanadate, and 1% w/v Triton X-100 (pH 7.4). The final pellet was resuspended in 50 μl Laemmli buffer, boiled for 5 min, and stored at −20° C until electrophoresis.

2.6. Immunoblotting

Immunoblotting was performed as previously described (Muñoz et al., 2009; 2017; Quiroga et al., 2018). Briefly, homogenized tissue proteins were transferred to PVDF membranes and blotted with anti-phospho-Akt, or anti-phospho-ERK1/2 antibodies (1:2000 dilution for all antibodies). Immunoprecipitated IR samples were subjected to immunoblotting with either a specific anti-phosphotyrosine or with the same antibody used for immunoprecipitation to determine protein abundance of the IR. The abundance of Akt, and ERK1/2 was detected in tissue lysates using the corresponding anti-protein antibodies at 1:2000 dilution. The abundance of adiponectin and UCP-1 in adipose tissue was detected in tissue lysates using specific antibodies at 1:1000 dilution. ECL and Hyperfilm (ThermoFisher Scientific, Waltham, MA, USA) were used to detect proteins. Bands were quantified using Gel-Pro Analyzer 4.0 (Media Cybernetics, Bethesda, MD, USA). Equal protein loading was controlled by staining the developed membranes with Coomasie blue. Additionally, the content of β-actin in solubilized protein extracts was used as a loading control and was assessed in independent inmunoblottings using the same volume of samples used for determination of the phosphorylation and content of insulin signaling molecules by incubation with an anti- β-actin antibody. Representative images are shown in Supplementary Figure 1.

2.7. Determination of circulating adiponectin, insulin, triglycerides and cholesterol levels

Serum cholesterol and triglycerides were measured with enzymatic colorimetric assay kits (Wiener Lab, Rosario, Argentina). Serum insulin and adiponectin levels were assessed by ELISA using the ultrasensitive mouse insulin ELISA (catalog 90080) and mouse adiponectin ELISA kit (catalog 80569) from Crystal Chem (Downers Grove, IL, USA).

The homeostasis model assessment of basal insulin resistance (HOMA-IR) was used to calculate an index from the product of the fasting concentrations of serum glucose (mmol/l) and serum insulin (μU/ml) divided by 22.5 (Matthews et al., 1985). Lower HOMA-IR values indicated greater insulin sensitivity, whereas higher HOMA-IR values indicated lower insulin sensitivity (insulin resistance).

2.8. Statistical Analysis

Values are reported as means ± SEM unless specified otherwise. Statistical significance was determined by one-way ANOVA (for comparison of data obtained from the ITT and GTT); Student's t-test (for comparison of the areas under the curve obtained during the ITT and GTT as well as adiponectin and UCP-1 abundance), or two-way ANOVA followed by Tukey's multiple comparison post hoc test (for comparison of metabolic parameters and insulin signaling pathways activation between groups). Differences were assigned significance at P< 0.05. All analyses were performed using GraphPad Prism 8 (GraphPad Software, San Diego, CA, USA).

3. Results

3.1 AT2R deletion impairs insulin sensitivity in female mice but not in male mice.

Body weight of both female WT and AT2RKO mice was significantly lower when compared to the corresponding male mice (Table 1). Deletion of the AT2R did not affect body weight regardless of sex. Serum glucose levels were numerically lower in both female WT and AT2RKO mice when compared to the respective group of male mice. However, this change did not reach statistical significance (Table 1). When compared to female WT mice, insulin sensitivity was impaired in female AT2RKO mice (Fig. 1A and B; (curve nadir: 44 ± 4% of initial glucose in female AT2RKO mice vs. 23 ± 17% of initial glucose in female control mice). The area under the curve for the ITT was significantly higher in female AT2RKO mice (7193 ± 1216) compared to the female WT group (5465 ± 1315; P < 0.05; Fig. 1B). Remarkably, male AT2RKO mice displayed unaltered insulin sensitivity when compared to male WT animals (Fig. 1C and 1D). Glucose handling in both female and male AT2RKO mice was evaluated in a GTT (Fig. 2A–D). When compared to the corresponding WT group, changes in blood glucose levels during the test where similar in AT2RKO mice of either sex (Fig. 2A and 2C). In consequence, the area under the curve for the GTT was not significantly different from the corresponding WT group either in female AT2RKO (Fig. 2B) or male AT2RKO mice (Fig. 2D), indicating that global deletion of the AT2R does not modify glucose tolerance. Although insulin sensitivity was impaired in female AT2RKO mice, this alteration coincided with statistically unaltered circulating levels of insulin, cholesterol and triglycerides (Table 1). Male ATR2KO mice show similar values for the metabolic parameters analyzed, (Table 1). Although changes in glucose and insulin

circulating values between AT2RKO and WT mice were non-significant, the HOMA score was calculated for an enhanced characterization of changes in the glycemic profile of these animals. As shown in Table 1, when compared with female WT mice, there was a tendency to an increase in the HOMA score in AT2RKO female mice indicative of a deterioration of the glycemic profile after global AT2R deletion (Table 1), while this change was not significant. No apparent changes were found for male mice.

Circulating levels of adiponectin were decreased in female WT mice as compared to male WT mice (P<0,01; Table 1). Deletion of the AT2R generated an increase in serum adiponectin levels in female mice, reaching levels that were comparable to those detected in male WT mice (Table 1). In contrast, global deletion of the AT2R did not affect circulating levels of adiponectin in male mice (Table 1).

3.2 The impairment of insulin sensitivity in female AT2RKO mice correlates with decreased activation of essential insulin signaling molecules in adipose tissue.

Decreased insulin sensitivity in female AT2RKO mice was associated with a significant impairment in insulin signaling in adipose tissue (Fig. 3–5). Insulin-induced phosphorylation levels of the insulin receptor (IR) at Tyr residues 1158/1162/1163 were reduced to 47% (P < 0.01) in adipose tissue of female insulin-stimulated AT2RKO mice, compared to values detected in female insulin-stimulated WT mice (Fig. 3A). No apparent differences in insulin-stimulated phosphorylation of the IR in liver (Fig. 3C) or skeletal muscle (Fig. 3E) were detected between female wild-type and AT2RKO mice. In addition, insulin-induced phosphorylation levels of Akt were significantly reduced to 59% at Ser473 (P < 0.01), in adipose tissue of female insulin-stimulated AT2RKO mice, when compared to values obtained in insulin-stimulated female WT mice (Fig. 4A). Akt activation reached similar levels in liver (Fig. 4C) and skeletal muscle (Fig. 4E) of female AT2RKO mice and the respective WT group. The attenuation of insulin signaling in adipose tissue from female AT2RKO mice was also extended to ERK1/2 (Fig. 5A). An approximate 35% reduction in insulin-stimulated ERK1/2 phosphorylation at Thr202/Tyr204 residues was observed in this tissue (Fig. 5A). ERK1/2 phosphorylation in either liver (Fig. 5C) and skeletal muscle (Fig. 5E) was not affected in female insulin-stimulated AT2RKO mice.

In contrast to changes observed in female animals, male AT2RKO mice displayed unaltered insulin-stimulated phosphorylation levels of the IR (Fig. 3B, 3D and 3F) and Akt (Fig. 4B, 4D. and 4F) when compared to values detected in WT male mice. Although not statistically significant, there were some alterations in ERK/1/2 phosphorylation in AT2RKO male mice (Fig. 5B, 5D and 5F). In particular, when compared to levels observed in WT male mice, insulin-stimulated ERK1/2 phosphorylation tended to be lower in adipose tissue from AT2RKO mice (Fig. 5B; P = 0.08 vs. WT mice). In addition, basal ERK1/2 phosphorylation was numerically higher in liver from AT2RKO male mice (Fig. 5D). ERK1/2 phosphorylation reached comparable levels in skeletal muscle from AT2RKO and WT male mice (Fig. 5F).

Protein abundance of the signaling molecules analyzed was not significantly changed in AT2RKO mice as compared to their WT counterparts (Fig. 3–5).

3.3   Adiponectin and UCP-1 levels are unaltered in perigonadal adipose tissue from AT2RKO mice.

Perigonadal levels of adiponectin were not significantly altered by the deletion of the AT2R in either sex (Fig. 6A and 6B), although there was a tendency to an increase of adiponectin levels in AT2RKO female mice when compared to the corresponding WT values (Fig. 6A). UCP-1 abundance in perigonadal adipose tissue was not significantly affected by the global deletion of the AT2R regardless of sex (Fig. 6C and 6D).

4.   Discussion

The main finding of these studies is that deletion of the AT2R decreased insulin sensitivity in female mice as opposed to male mice that shown no alterations. Interestingly, when compared to female WT mice, we have also observed that female AT2RKO mice had a tissue-specific reduction in the response to insulin of the main signaling components, namely IR, Akt and ERK1/2 in adipose tissue. In contrast, the insulin signaling response of the female AT2RKO mice was similar in both liver and skeletal muscle as compared to female WT mice. In line with the sex-specific difference observed in terms of insulin sensitivity, we found that insulin-induced phosphorylation levels of the IR, Akt and ERK1/2 in male AT2RKO mice were unaltered as compared to WT males. Collectively, these data demonstrate a sexual dimorphism of AT2R deletion on insulin sensitivity in mice, with a negative impact only in females compared with males.

Together with the ACE2-Ang-(1–7)-Mas receptor pathway, the Ang II-AT2R pathway is viewed as counterregulatory of classic ACE-AngII-AT1R arm of the RAS. A large set of data has been accumulated in favor of a physiological role of AT2R on glucose homeostasis (Chai et al., 2010; Chai et al., 2011; Leung et al., 2014; Muñoz et al., 2017; Ohshima et al., 2012; Quiroga et al.; 2018; Shao et al., 2014; Than et al., 2017; Wang et al., 2017; Yan et al., 2018). In this scenario, pharmacologic manipulation aimed at increasing the AT2R-to-AT1R activity ratio may have the potential to enhance insulin sensitivity and glucose metabolism and to diminish the cardiovascular complications associated with diabetes and insulin resistance (Paulis et al., 2016). In particular, recent reports have shown that pharmacological stimulation of the AT2R with compound 21 induces an improvement of insulin action in different rodent models of insulin resistance and type 2 diabetes, including KK-Ay diabetic mice (Ohshima et al., 2012), high-fat/high-fructose fed rats (Shum et al., 2013), STZ-diabetic rats (Shao et al., 2014; Wang et al., 2017), and Zucker diabetic fatty rats (Castoldi et al., 2014). In addition, we have recently shown that stimulation of AT2R improves insulin sensitivity in normal C57Bl/6 mice (Quiroga et al., 2018). The mechanisms by which AT2R stimulation favors insulin sensitivity appear to involve augmentation of plasma adiponectin levels (Ohshima et al., 2012; Quiroga et al., 2018; Than et al., 2017), enhancement of insulin production (Shao et al., 2013; 2014) and protection of pancreatic β-cells from oxidative stress (Shao et al., 2014; Wang et al., 2017). In addition, involvement of AT2R in physiological stimulation of T3-induced white adipose browning has been recently suggested (Than et al., 2017). Research of mice with genetic deletion of the AT2R lead to a disparity of results (Noll et al., 2015; Samuel et al., 2013; Shiuchi et al., 2004; Yvan-Charvet et al., 2005).

Our current findings showing that insulin sensitivity is impaired after disruption of the *Agtr2* gene in female mice, with no detectable influence in male animals, could be ascribed to the different levels of expression of AT2R detected in female versus male mice (Armando et al., 2002; Baiardi et al., 2005). Female mice have been shown to express renal AT2Rs in numbers substantially higher than those present in male mice (Armando et al., 2002). Estrogen seems to have a major role in this difference, since administration of this hormone has been shown to profoundly upregulate AT2R expression in the mouse kidney, altering the AT1R/AT2R expression ratio (Baiardi et al., 2005). In spontaneously hypertensive rats, greater renal AT2R mRNA gene expression has been reported in females as compared with males (Silva-Antonialli et al., 2004). The magnitude of the difference in AT2R mRNA expression between males and females in this study was almost 300-fold, indicating a shift in the balance between AT1R and AT2R toward increased AT2R in females (Silva-Antonialli et al., 2004). It has previously been shown that female, but not male AT2RKO are intolerant to glucose (Samuel et al., 2013). Sexual dimorphism in the physiological responses originated from the AT2R have been reported previously. Infusion of the AT2R antagonist PD123319 has been reported to promote greater renal injury after ischemia/reperfusion in female more than in male rats (Maleki et al., 2016.). Taking together, we hypothesize that the AT2R could be a greater contributor to insulin sensitivity modulation in female compared to male mice. Noteworthy, we have previously demonstrated that chronic treatment with C21 increases insulin sensitivity in male mice (Quiroga et al., 2018). However, this was achieved with a high dose of C21. It remains to be elucidated whether same beneficial effects can be achieved in female mice with lower doses of C21.

Shao et al., analyzed the abundance of the AT2R in several tissues of male rats by western blotting and found that the pancreas was one of the few tissues that contained a significant proportion of the AT2R as compared with that of AT1R. This agrees with results obtained in humans (Lam et al., 2002) and in larger animals (Chappell et al., 1992; 1994), in all suggesting a major role for pancreatic AT2R in the promotion of proinsulin gene expression, insulin protein biosynthesis, insulin secretion, and insulin action found after administration of male rats with C21 (Shao et al., 2013). In relation to our current study, unfortunately there is no available data on the relative expression of the AT2R to that of the AT1R in mice pancreas, or on the relative expression/binding activity of the AT2R in female versus male mice which appears as a very relevant study aspect.

Protein kinase B/Akt is a major mediator of insulin action (Boucher et al., 2014). Our current findings showed impaired insulin signaling in adipose tissue of AT2RKO mice, which are consistent with our previous works reporting impaired insulin signaling in adipose tissue after chronic blockade of the AT2R with PD123319 (Muñoz et al., 2017). In addition, we have recently demonstrated that administration of a high dose of compound 21 to C57Bl/6 mice results in a tissue-specific enhancement of insulin-stimulated Akt activation selectively in adipose tissue, while decreasing adipocyte size and increasing adiponectin expression in this tissue (Quiroga et al., 2018). In agreement with these results, previous studies reported a tissue-specific reduction of glucose uptake in AT2RKO mice with no apparent difference in insulin-mediated glucose uptake into skeletal muscle between WT and AT2RKO mice, and a significant reduction of insulin-induced glucose uptake in white adipose tissues in AT2RKO mice (Shiuchi et al., 2004). Together with this observation, our

current results and previous findings point to adipose tissue as the mostly affected site after *in vivo* AT2R stimulation, blockade or deletion in terms of insulin action.

Finally, previous studies from our lab have shown that blockade of the AT2R with PD12319 impairs insulin signaling in adipose tissue of males while activation of these receptors induces the opposite effect (Muñoz *et al.*, 2017, Quiroga *et al.*, 2018). In the current study, deletion of AT2R had no effect on insulin signaling in male adipose tissue but impaired the insulin signaling in female fat only. Regarding this difference between our current results and our previous study, blockade with PD123319 was attained only for one month and in AT2RKO the absence of AT2R is constant since birth. In addition, there are several sex dimorphisms in metabolic homeostasis, diabetes, and obesity. Female adipocytes have increased insulin sensitivity compared with male adipocytes (Guerre-Millo et al., 1985; Macotela et al., 2009). Also, female adipocytes have increased lipid synthesis compared with male adipocytes, and in females, perigonadal adipocytes also have improved insulin sensitivity to lipogenesis and to insulin signaling (Macotela et al., 2009). These contribute to the higher whole-body insulin sensitivity displayed by females (Macotela et al., 2009). These differences could have contributed to the effect of AT2R deletion found in the current study.

Results from Than et al. and our laboratory have indicated that stimulation of AT2R leads to an increase of the insulin-sensitizer hormone adiponectin and of UCP-1 in adipose tissue (Than et al., 2017; Quiroga et al., 2018). To further characterize the effects of AT2R deletion, we measured adiponectin and UCP-1 in perigonadal adipose tissue and found no apparent changes between KO and WT animals of either sex. Adiponectin levels were found to be significantly lower in female WT mice than in female AT2RKO mice. This could represent a compensatory mechanism in response to decreased insulin sensitivity. The fact that female AT2RKO mice presented impair insulin tolerance despite displaying higher circulating levels than WT animals could be indicative of adiponectin resistance as has been described for other models (Engin, 2017). The absence of modification in the levels of UCP-1 in AT2RKO mice contrasts with the previously reported increased levels of this protein after pharmacological activation of the AT2R in normal mice (Than et al., 2017; Quiroga et al., 2018). Permanent deletion of the AT2R since birth is difficult to compare with a temporary activation of the AT2R, probably several compensatory changes are taking place in AT2RKO mice and this leads to normalization of UCP-1 levels.

Conclusions

In the current study we show that AT2RKO mice display both a sex- and tissue-specific reduction of insulin action. Insulin sensitivity is impaired in female AT2RKO mice, while their male counterparts display a normal phenotype in terms of insulin sensitivity. Impairment of insulin sensitivity in female AT2RKO mice is associated with an attenuation of the activation of main insulin signaling components, namely, IR, Akt and ERK1/2 selectively in adipose tissue. These results together with our previous reports in which the AT2R was pharmacologically blocked or activated, suggest that the presence of the AT2R in adipose tissue is critical to the role of this receptor in the control of insulin action and glucose homeostasis.

Supplementary Material

Refer to Web version on PubMed Central for supplementary material.

Abbreviations

Ang II	angiotensin II
AT1R	angiotensin II type 1 receptor
AT2R	angiotensin II type 2 receptor
C21	compound 21
ERK	extracellular signal-regulated kinase
GTT	glucose tolerance test
IR	insulin receptor
ITT	insulin tolerance test
KO	knockout
RAS	renin angiotensin system
WAT	white adipose tissue
WB	western blotting
WT	wild-type

References

Altarche-Xifró W, Curato C, Kaschina E, Grzesiak A, Slavic S, Dong J, et al., 2009 Cardiac c-kit +AT2+ cell population is increased in response to ischemic injury and supports cardiomyocyte performance. Stem Cells 27, 2488–2497. [PubMed: 19591228]

Armando I, Jezova M, Juorio AV, Terrón JA, Falcón-Neri A, Semino-Mora C, et al., 2002 Estrogen upregulates renal angiotensin II AT2 receptors. Am. J. Physiol. Renal Physiol 283, F934–F943. [PubMed: 12372768]

Baiardi G, Macova M, Armando I, Ando H, Tyurmin D, Saavedra JM, 2005 Estrogen upregulates renal angiotensin II AT1 and AT2 receptors in the rat. Regul. Pept 124, 7–17. [PubMed: 15544836]

Boucher J, Kleinridders A, Kahn CR, 2014 Insulin receptor signaling in normal and insulin-resistant states. Cold Spring Harb. Perspect. Biol 6, a009191. [PubMed: 24384568]

Busche S, Gallinat S, Bohle RM, Reinecke A, Seebeck J, Franke F, et al., 2000 Expression of angiotensin AT(1) and AT(2) receptors in adult rat cardiomyocytes after myocardial infarction, A single-cell reverse transcriptase-polymerase chain reaction study. Am. J. Pathol 157, 605–611. [PubMed: 10934163]

Carey RM, 2017 Update on angiotensin AT2 receptors. Curr. Opin. Nephrol. Hypertens 26, 91–96. [PubMed: 27906747]

Castoldi G, di Gioia CR, Bombardi C, Maestroni S, Carletti R, Steckelings UM et al., 2014 Prevention of diabetic nephropathy by compound 21, selective agonist of angiotensin type 2 receptors, in Zucker diabetic fatty rats. Am. J. Physiol. Renal Physiol 307, F1123–F1131. [PubMed: 25186297]

Chai W, Wang W, Dong Z, Cao W, Liu Z, 2011 Angiotensin II receptors modulate muscle microvascular and metabolic responses to insulin in vivo. Diabetes 60, 2939–2946. [PubMed: 21896931]

Chai W, Wang W, Liu J, Barrett EJ, Carey RM, Cao W, et al., 2010 Angiotensin II type 1 and type 2 receptors regulate basal skeletal muscle microvascular volume and glucose use. Hypertension 55, 523–530. [PubMed: 19996061]

Chappell MC, Bosch SM, Hansen BC, Ferrario CM, Diz DI, 1994 Differential expression of AT2 angiotensin II receptors in the primate pancreas (Abstract). J. Hypertension 12, S181.

Chappell MC, Diz DI, Jacobsen DW, 1992 Pharmacological characterization of angiotensin II binding sites in the canine pancreas. Peptides 13, 313–318. [PubMed: 1409010]

Engin A, 2017 Adiponectin-resistance in obesity. Adv. Exp. Med. Biol 960, 415–441. [PubMed: 28585210]

Forrester SJ, Booz GW, Sigmund CD, Coffman TM, Kawai T, Rizzo V, et al., 2018 Angiotensin II signal transduction: an update on mechanisms of physiology and pathophysiology. Physiol. Rev 98, 1627–1738. [PubMed: 29873596]

Gallinat S, Yu M, Dorst A, Unger T, Herdegen T, 1998 Sciatic nerve transection evokes lasting up-regulation of angiotensin AT2 and AT1 receptor mRNA in adult rat dorsal root ganglia and sciatic nerves. Brain Res. Mol. Brain Res 57, 111–122. [PubMed: 9630555]

Guerre-Millo M, Leturque A, Girard J, Lavau M, 1985 Increased insulin sensitivity and responsiveness of glucose metabolism in adipocytes from female versus male rats. J. Clin. Invest 76, 109–116. [PubMed: 3894416]

Henriksen EJ, Jacob S, Kinnick TR, Teachey MK, Krekler M, 2001 Selective angiotensin II receptor antagonism reduces insulin resistance in obese Zucker rats. Hypertension 38, 884–890. [PubMed: 11641303]

Ichiki T, Labosky PA, Shiota C, Okuyama S, Imagawa Y, Fogo A, et al., 1995 Effects on blood pressure and exploratory behaviour of mice lacking angiotensin II type-2 receptor. Nature 377, 748–750. [PubMed: 7477267]

Karnik SS, Unal H, Kemp JR, Tirupula KC, Eguchi S, Vanderheyden PM, et al., 2015 International Union of Basic and Clinical Pharmacology. XCIX. Angiotensin receptors: interpreters of pathophysiological angiotensinergic stimulis. Pharmacol. Rev 67, 754–819. [PubMed: 26315714]

Lam KY, Leung PS, 2002 Regulation and expression of a renin–angiotensin system in human pancreas and pancreatic endocrine tumours. Eur. J. Endocrinol 146: 567–572. [PubMed: 11916627]

Leung KK, Liang J, Zhao S, Chan WY, Leung PS, 2014 Angiotensin II type 2 receptor regulates the development of pancreatic endocrine cells in mouse embryos. Dev. Dyn 243, 415–427. [PubMed: 24166718]

Li J, Culman J, Hörtnagl H, Zhao Y, Gerova N, Timm M, et al., 2005 Angiotensin AT2 receptor protects against cerebral ischemia-induced neuronal injury. FASEB J. 19, 617–619. [PubMed: 15665034]

Macotela Y, Boucher J, Tran TT, Kahn CR, 2009 Sex and depot differences in adipocyte insulin sensitivity and glucose metabolism. Diabetes 58, 803–812. [PubMed: 19136652]

Maleki M, Nematbakhsh M, 2016 Gender difference in renal blood flow response to angiotensin II administration after ischemia/reperfusion in rats: the role of AT2 receptor. Adv. Pharmacol. Sci 2016, 7294942. [PubMed: 27034657]

Matavelli LC, Siragy HM, 2015 AT2 receptor activities and pathophysiological implications. Cardiovasc. Pharmacol 65, 226–232.

Matthews DR, Hosker JP, Rudenski AS, Naylor BA, Treacher DF, Turner RC, 1985 Homeostasis model assessment: insulin resistance and beta cell function from fasting plasma glucose and insulin concentrations in man. Diabetologia 28, 412–419. [PubMed: 3899825]

Muñoz MC, Burghi V, Miquet JG, Cervino IA, Quiroga DT, Mazziotta L, et al., 2017 Chronic blockade of the AT2 receptor with PD123319 impairs insulin signaling in C57BL/6 mice. Peptides 88, 37–45. [PubMed: 27979738]

Muñoz MC, Giani JF, Dominici FP, Turyn D, Toblli JE, 2009 Long-term treatment with an angiotensin II receptor blocker decreases adipocyte size and improves insulin signaling in obese Zucker rats. J. Hypertens 27, 2409–2420. [PubMed: 19901849]

Nakajima M, Hutchinson HG, Fujinaga M, Hayashida W, Morishita R, Zhang L, et al., 1995 The angiotensin II type 2 (AT2) receptor antagonizes the growth effects of the AT1 receptor: gain-of-function study using gene transfer. Proc. Natl. Acad. Sci. U.S.A 92, 10663–10667. [PubMed: 7479861]

Nio Y, Matsubara H, Murasawa S, Kanasaki M, Inada M, 1995 Regulation of gene transcription of angiotensin II receptor subtypes in myocardial infarction. J. Clin. Invest 95, 46–54. [PubMed: 7814645]

Noll C, Labbé SM, Pinard S, Shum M, Bilodeau L, Chouinard L, et al., 2015 Postprandial fatty acid uptake and adipocyte remodeling in angiotensin type 2 receptor-deficient mice fed a high-fat/high-fructose diet. Adipocyte 5, 43–52. [PubMed: 27144096]

Ohshima K, Mogi M, Jing F, Iwanami J, Tsukuda K, Min LJ, et al., 2012 Direct angiotensin II type 2 receptor stimulation ameliorates insulin resistance in type 2 diabetes mice with PPARγ activation. PLoS One 7, e48387. [PubMed: 23155382]

Paulis L, Foulquier S, Namsolleck P, Recarti C, Steckelings UM, Unger T, 2016 Combined angiotensin receptor modulation in the management of cardio-metabolic disorders. Drugs 76, 1–12. [PubMed: 26631237]

Quiroga DT, Muñoz MC, Gil C, Pffeifer M, Toblli JE, Steckelings UM, et al., 2018 Chronic administration of the angiotensin type 2 receptor agonist C21 improves insulin sensitivity in C57BL/6 mice. Physiol. Rep 6, e13824. [PubMed: 30156060]

Rodriguez R, Minas JN, Vazquez-Medina JP, Nakano D, Parkes DG, Nishiyama A, et al., 2018 Chronic AT1 blockade improves glucose homeostasis in obese OLETF rats. J. Endocrinol 237, 271–284. [PubMed: 29643115]

Saiki A, Ohira M, Endo K, Koide N, Oyama T, Murano T, 2009 Circulating angiotensin II is associated with body fat accumulation and insulin resistance in obese subjects with type 2 diabetes mellitus. Metabolism 58, 708–713. [PubMed: 19375596]

Samuel P, Khan MA, Nag S, Inagami T, Hussain T, 2013 Angiotensin AT(2) receptor contributes towards gender bias in weight gain. PLoS One 8, e48425. [PubMed: 23341867]

Santos RAS, Oudit GY, Verano-Braga T, Canta G, Steckelings UM, Bader M, 2019 The renin-angiotensin system: going beyond the classical paradigms. Am. J. Physiol. Heart. Circ. Physiol 316, H958–H970. [PubMed: 30707614]

Shao C, Yu L, Gao L, 2014 Activation of angiotensin type 2 receptors partially ameliorates streptozotocin-induced diabetes in male rats by islet protection. Endocrinology 155, 793–804. [PubMed: 24302627]

Shao C, Zucker IH, Gao L, 2013 Angiotensin type 2 receptor in pancreatic islets of adult rats: a novel insulinotropic mediator. Am. J. Physiol. Endocrinol. Metab 305, E1281–1291. [PubMed: 24085035]

Shiuchi T, Iwai HS Li L Wu LJ Min JM Li M, et al., 2004 Angiotensin II type-1 receptor blocker valsartan enhances insulin sensitivity in skeletal muscles of diabetic mice. Hypertension 43, 1003–1010. [PubMed: 15037562]

Shum M, Pinard S, Guimond MO Labbé SM, Roberge C, Baillargeon JP, et al., 2013 Angiotensin II type 2 receptor promotes adipocyte differentiation and restores adipocyte size in high-fat/high-fructose diet-induced insulin resistance in rats. Am. J. Physiol. Endocrinol. Metab 304, E197–E210. [PubMed: 23149621]

Silva-Antonialli MM, Tostes RC Fernandes L, Fior-Chadi DR, Akamine EH, Carvalho MH, et al., 2004 A lower ratio of AT1/AT2 receptors of angiotensin II is found in female than in male spontaneously hypertensive rats. Cardiovasc. Res 62, 587–593. [PubMed: 15158151]

Steckelings UM, Rompe F, Kaschina E, Namsolleck P, Grzesiak A, Funke-Kaiser H, et al., 2010 The past, present and future of angiotensin II type 2 receptor stimulation. J. Renin-Angiotensin-Aldosterone Syst 11, 67–73. [PubMed: 19861348]

Than A, Xu S, Li R, Leow MS, Sun L, Chen P, 2017 Angiotensin type 2 receptor activation promotes browning of white adipose tissue and brown adipogenesis. Signal Transduct. Target Ther 2, 17022. [PubMed: 29263921]

Wang L Wang Y, Li XY, Leung P, 2017 Angiotensin II type 2 receptor activation with compound 21 augments islet function and regeneration in streptozotocin-induced neonatal rats and human pancreatic progenitor cells. Pancreas. 46, 395–404. [PubMed: 28099262]

Wang L, Wang Y, Li XY, Leung PS, 2017 Angiotensin II type 2 receptor activation with compound 21 augments islet function and regeneration in streptozotocin-induced neonatal rats and human pancreatic progenitor cells. Pancreas 46, 395–404. [PubMed: 28099262]

Yan F, Yuan Z, Wang N, Carey RM, Aylor KW, Chen L, et al., 2018 Direct activation of angiotensin II type 2 receptors enhances muscle microvascular perfusion, oxygenation, and insulin delivery in male rats. Endocrinology 159, 685–695. [PubMed: 29186390]

Yvan-Charvet L, Even P, Bloch-Faure M, Guerre-Millo M, Moustaid-Moussa N, Ferre P, et al., 2005 Deletion of the angiotensin type 2 receptor (AT2R) reduces adipose cell size and protects from diet-induced obesity and insulin resistance. Diabetes 54, 991–999. [PubMed: 15793237]

Highlights

- AT2RKO mice present a sexual dimorphism in terms of insulin sensitivity.

- AT2R deletion impairs insulin tolerance in female mice.

- AT2RKO does not affect insulin sensitivity in male mice.

- In female mice, AT2R deficiency leads to a selective attenuation of insulin signaling in adipose tissue.

- AT2R in adipose tissue appears to have a major role in the control of insulin action.
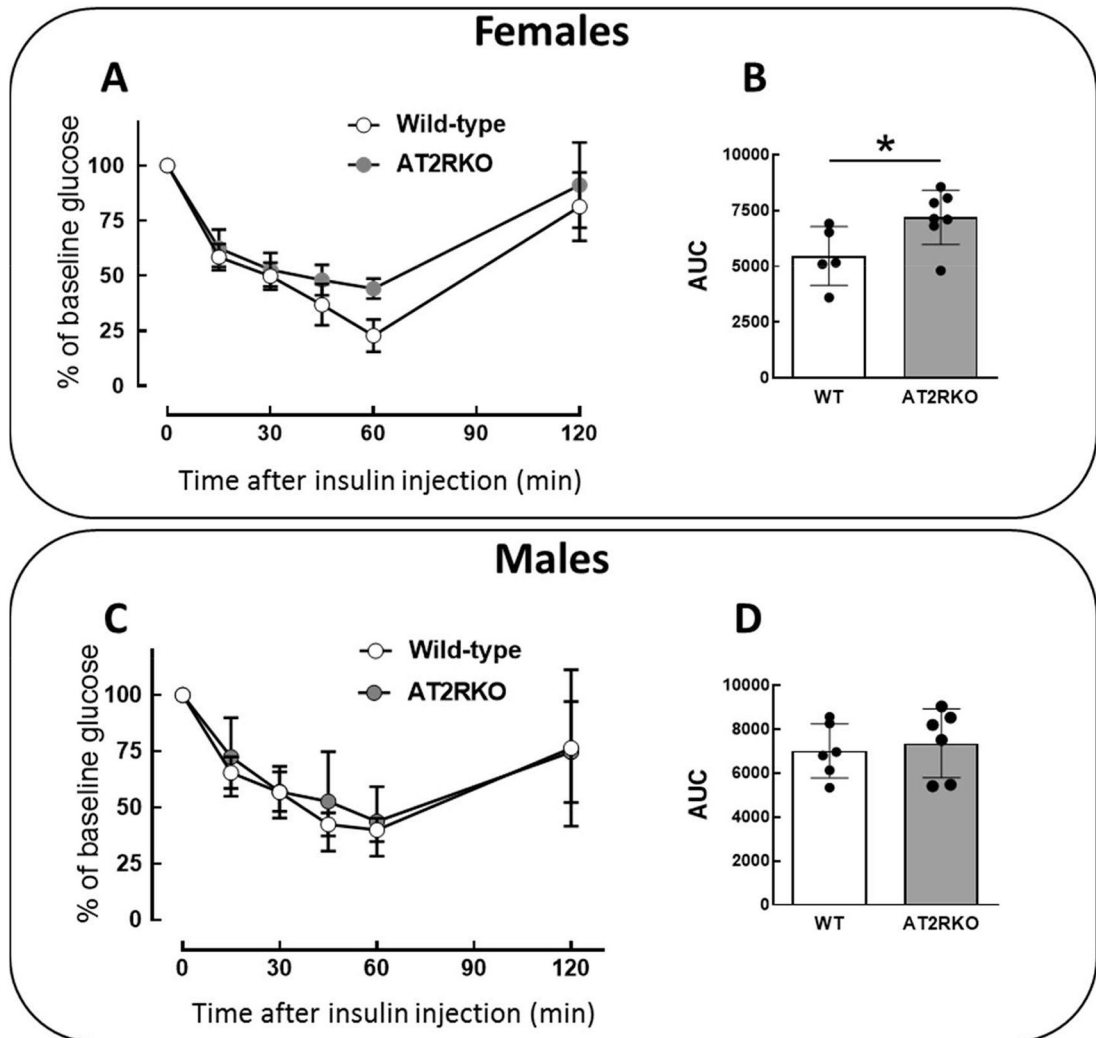
Insulin tolerance test

Fig. 1. -
Evaluation of insulin tolerance in AT2RKO (n=6 per group) and WT (n=6 per group) mice. Glucose levels during an insulin tolerance test (ITT) performed in female (Panel A) and male (Panel C) WT and AT2RKO mice. Panels B and D show the calculated area under the curve from the ITTs displayed in (A) and (C) respectively. Mice were fasted for 6 h prior to basal glucose monitoring (as described in Materials and Methods) and subsequently injected i.p. with a 20% glucose solution (w/v). Blood was reanalyzed at 15, 30, 45, 60, and 120 min post-injection. Data are means ± SD. Areas under the curves were analyzed by Student's T test.
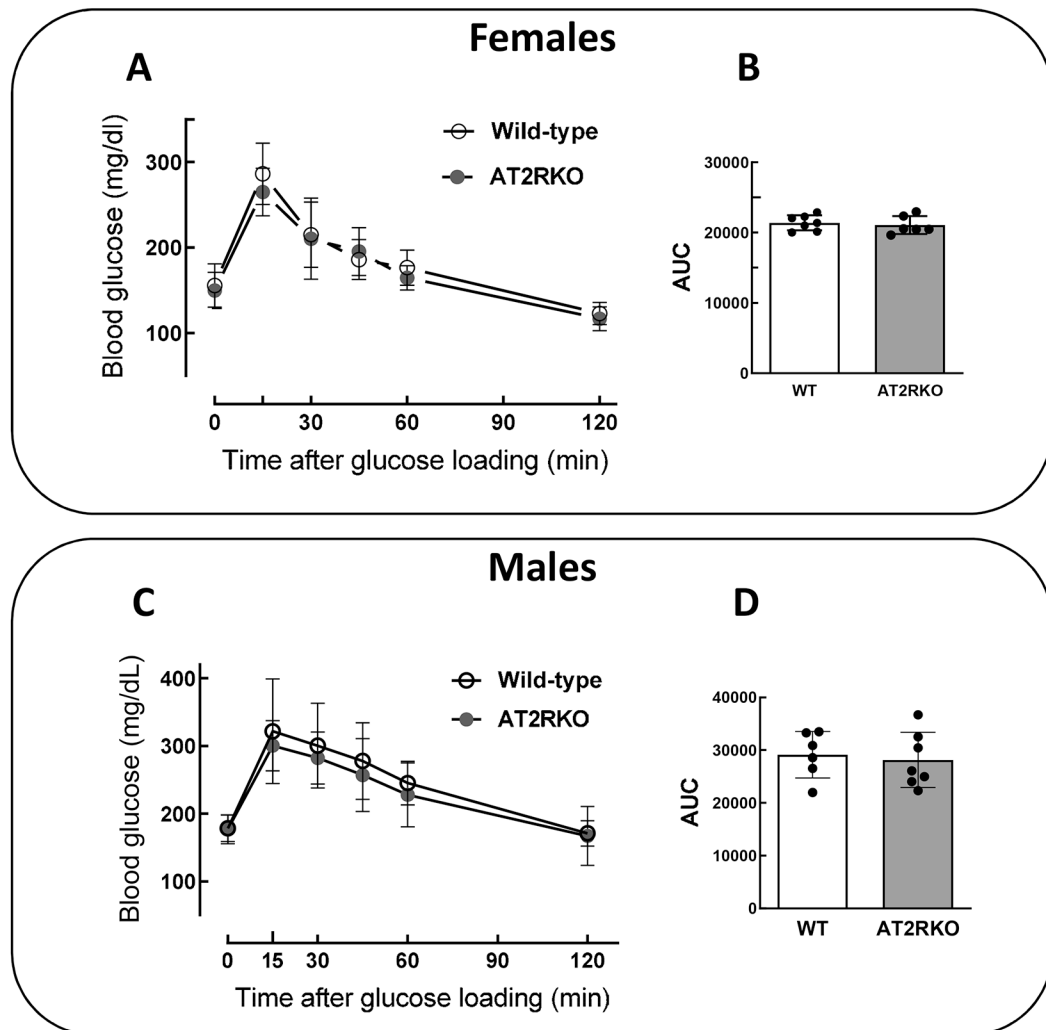
Glucose tolerance test

Fig. 2. -

Evaluation of glucose tolerance in AT2RKO (n=6 per group) and wild-type (WT; n=6 per group) mice. Glucose levels during a glucose tolerance test (GTT) performed in female (Panel A) and male (Panel C) WT and AT2RKO mice. Panels B and D show the calculated area under the curve from the GTTs displayed in (A) and (C) respectively. Mice were fasted for 6 h prior to basal glucose monitoring (as described in Materials and Methods) and subsequently injected i.p. with a 20% glucose solution (w/v). Blood was reanalyzed at 15, 30, 45, 60, and 120 min post-injection. Data are means ± SD. Areas under the curves were analyzed by Student's T test, where *P<0.05 vs. control mice.
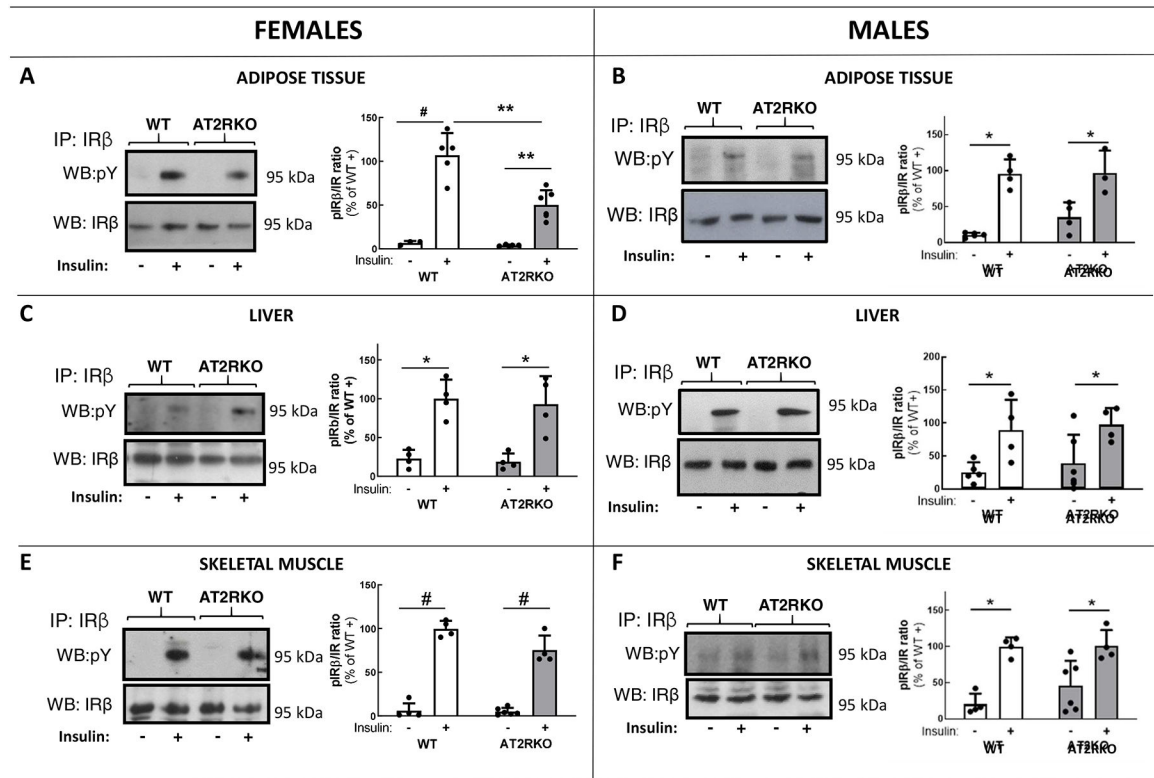
INSULIN RECEPTOR

Fig. 3. –.

Representative Western blot (WB) images and scattered plots A)–F) depicting fold change in insulin receptor (IR) tyrosine phosphorylation in main insulin target tissues of female (A, C, E) and male (B, D, F) WT and AT2RKO mice. Tyrosine (Y) phosphorylation levels was determined after acute injection with insulin (+) or vehicle (−) using an anti-phosphotyrosine antibody (pY) in samples that had been previously immunoprecipitated (IP) with an anti-IRβ antibody as described in Materials and Methods. IRβ subunit abundance was detected with the same antibody used for IP. Bar graphs represent the quantification of phosphorylated IR related to IRβ abundance. Data are mean ± SEM and are expressed as % of the insulin-stimulated WT mean value. Statistical significance was analyzed by two-way ANOVA followed by Tukey's multiple comparison t tests; n=5 in all cases. [(*) P < 0.05; (**) P < 0.01; (#) P < 0.001]
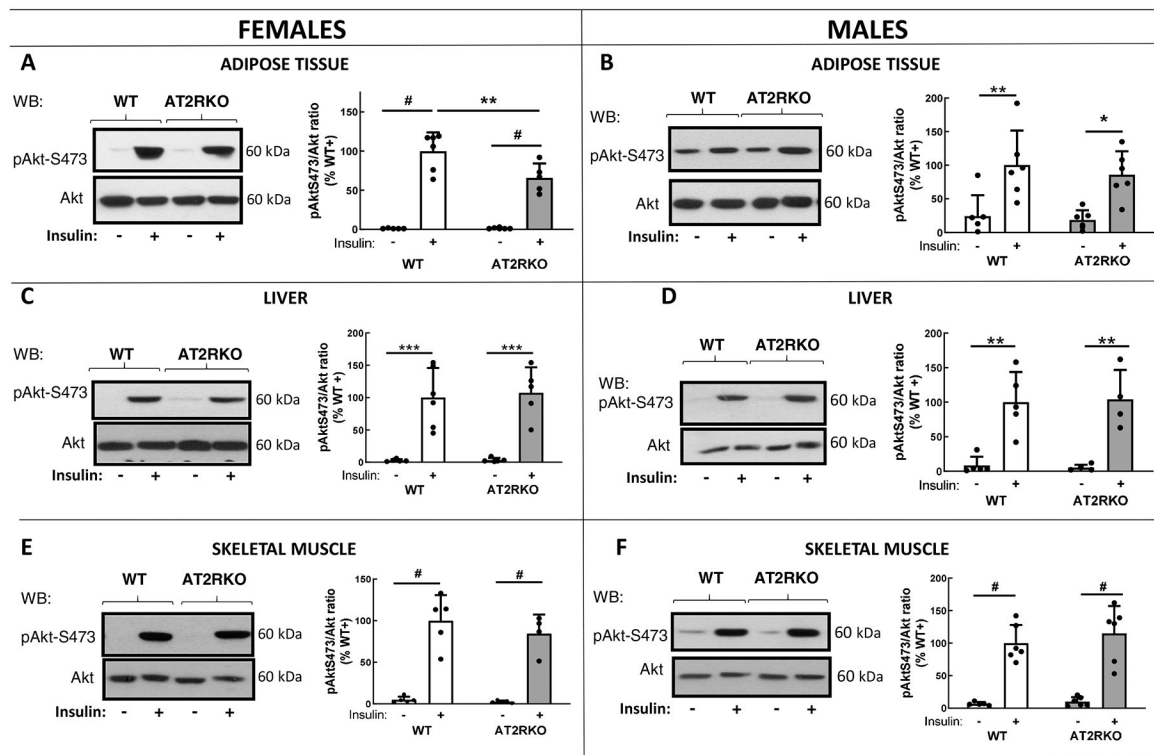
Akt

Fig. 4. –.

Representative Western blot (WB) images and scattered plots A)–F) depicting fold change in Akt phosphorylation in main insulin target tissues of female (A, C, E) and male (B, D, F) WT and AT2RKO mice. Specific antibodies were used to detect phosphorylation of Akt at Serine (S) 473. Total Akt was used as a loading control to normalise protein amount. Bar graphs represent the quantification of phosphorylated Akt related to Akt abundance. Data are mean ± SEM and are expressed as % of the insulin-stimulated WT mean value. Statistical significance was analyzed by two-way ANOVA followed by Tukey's multiple comparison t tests; n=5 in all cases. [(*) P < 0.05; (**) P < 0.01; (#) P < 0.001; (***) P < 0.0001].
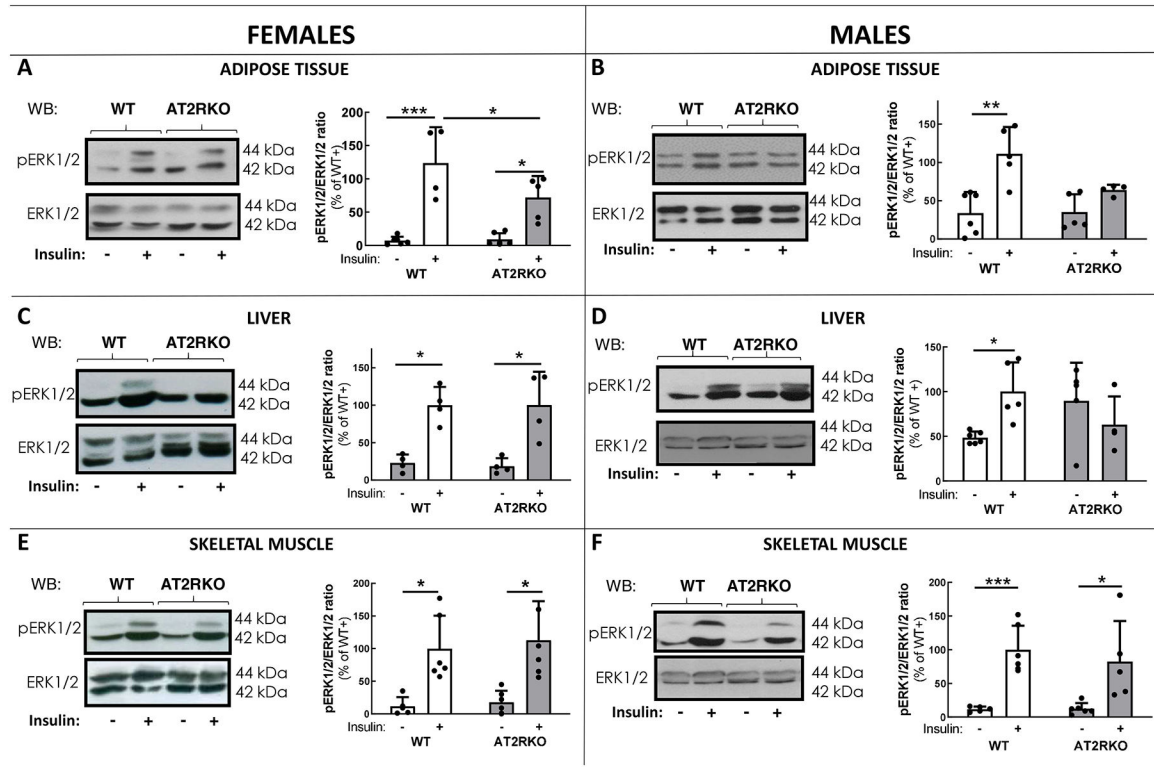
ERK1/2

Fig. 5. –.

Representative Western blot (WB) images and scattered plots A)–F) depicting fold change in ERK1/2 phosphorylation at activating residues Threonine 202 and Tyrosine 204 in main insulin target tissues of female (A, C, E) and male (B, D, F) WT and AT2RKO mice. Specific antibodies were used to detect phosphorylation of ERK1/2 at Threonine (Thr) 202 and Tyrosine (Tyr) 204. Total ERK1/2 was used as a loading control to normalise protein amount. Bar graphs represent the quantification of phosphorylated ERK1/2 related to ERK1/2 abundance. Data are mean ± SEM and are expressed as % of the insulin-stimulated WT mean value. Statistical significance was analyzed by two-way ANOVA followed by Tukey's multiple comparison t tests; n=5 in all cases. [(*) $P < 0.05$; (**) $P < 0.01$; (***) $P < 0.0001$].
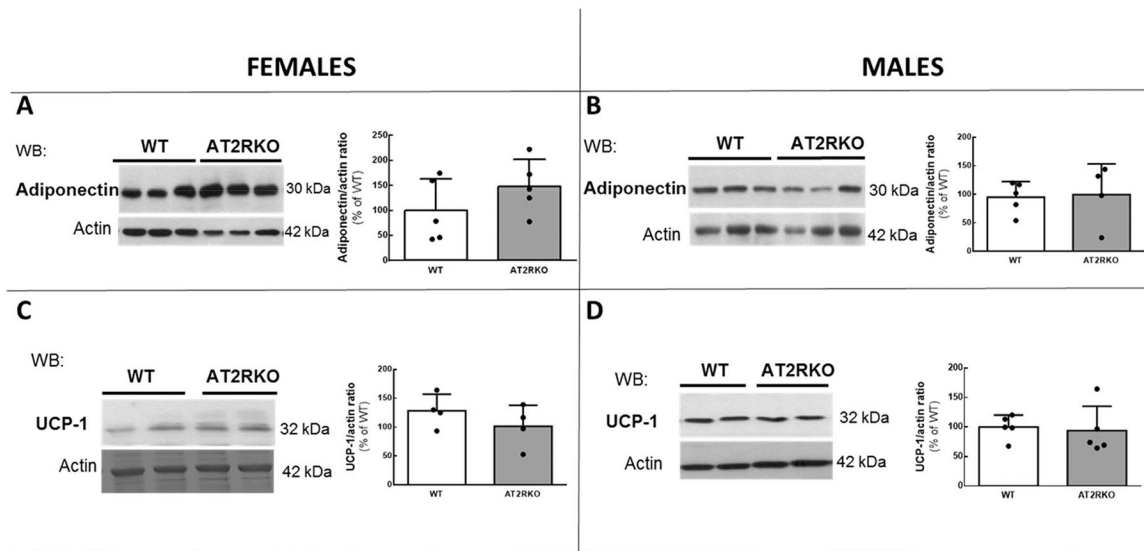
Fig. 6. –.

Representative Western blot (WB) images and scattered plots A)–D) depicting adiponectin (A and B) and UCP-1 abundance (C and D) in perigonadal adipose tissue from WT and AT2RKO mice. Actin was used as a loading control to normalise protein amount. For these determinations only samples of tissues from vehicle-injected samples were analyzed. Bar graphs represent the quantification of adiponectin and UCP-1 related to actin abundance. Data are mean ± SD and are expressed as % of the corresponding WT mean value. Statistical significance was analyzed by analyzed by Student's T test; n=5–6 per group.

Table 1

Characteristics of the experimental animals.

Animals were fasted for 6 h prior to blood extraction. Metabolic parameters were determined in serum from vehicle-treated animals. Serum cholesterol and triglycerides were measured with enzymatic colorimetric assay kits. Serum insulin and adiponectin levels were assessed using specific mouse insulin and adiponectin ELISA kits. HOMA, homeostasis model assessment.

Values are means ± SD. The number of samples used for each determination (n) is shown in parentheses. Data where compared by two-way ANOVA; *$P < 0.05$ when compared to the respective group of male mice; **$P < 0.01$ compared to all experimental groups.

Gender	Males		Females	
Type of animal	Wild-type	AT2RKO	Wild-type	AT2RKO
Body Weight (g)	27 ± 2 (7)	28 ± 1 (7)	20 ± 1* (6)	21 ± 1* (7)
Glucose (mg/dl)	178 ± 20 (7)	177 ± 21 (7)	156 ± 25 (7)	148 ± 20 (7)
Triglycerides (mg/dl)	24 ± 10 (6)	25 ± 8 (5)	38 ± 12 (6)	37 ± 13 (6)
Cholesterol (mg/dl)	66 ± 18 (6)	62 ± 11 (6)	61 ± 19 (6)	45 ± 11 (6)
Insulin (ng/ml)	2.6 ± 0.7 (6)	2.8 ± 0.8 (5)	2.3 ± 0.3 (5)	3.5 ± 1.0 (5)
Adiponectin (μg/ml)	24 ± 7 (8)	27 ± 8 (7)	12 ± 5# (8)	25 ± 5 (6)
HOMA score	2.8 ± 0.5 (6)	3.0 ± 0.6 (5)	2.2 ± 0.30 (5)	3.2 ± 0.6 (5)